Journal of Computational Physics **153,** 82–100 (1999)
Article ID jcph.1999.6265, available online at http://www.idealibrary.com on IDEAL®

Mixed Spectral-Boundary Element Embedding Algorithms for the Navier–Stokes Equations in the Vorticity-Stream Function Formulation

M. Elghaoui and R. Pasquetti

Laboratoire J. A. Dieudonné, UMR CNRS 6621, Université de Nice Sophia-Antipolis, Parc Valrose, 06108 Nice Cedex 2, France

Received October 27, 1998; revised March 18, 1999

An embedding approach, based on Fourier expansions and boundary integral equations, is applied to the vorticity-stream function formulation of the Navier–Stokes equations. The algorithm only requires efficient solvers of scalar elliptic equations and, in an asymptotic version, the boundary element method is only needed to solve the Laplace equation. The capabilities of this embedding method, in both its full and asymptotic versions, are pointed out by considering the classical problem of the flow between two eccentric cylinders.

1. INTRODUCTION

An attractive way to solve partial differential equations in geometries of complex shape consists in the use of embedding methods: the complex shaped domain is embedded in a cartesian geometry for which efficient solvers are available. Many approaches have already been suggested. Especially, one has to mention some earlier works [1, 2], some more recent approaches [3, 4], and also those developed by Glowinsky and co-workers (see, e.g., [5–7]), generally based on the use of a Lagrange multiplier defined on the boundary of the complex domain to enforce the boundary conditions.

The idea that we have developed more recently [8, 9] is based on the splitting of the original problem into two sub-problems, which are solved using a Fourier spectral method in the cartesian geometry and a boundary element method to fulfill the boundary conditions. Similar approaches were also suggested in [10, 11]. Let us recall the proposed algorithm for the following problem: find u, in the bounded domain Ω such as

$$\begin{aligned} Lu &= f \qquad \text{in } \Omega \\ \mathcal{B}(u) &= g \qquad \text{on } \Gamma = \partial\Omega, \end{aligned}$$

0021-9991/99 $30.00

where L is an elliptic differential operator (e.g., $L = \Delta - \sigma^2$) and $\mathcal{B}$ is a linear operator defined on $\Gamma = \partial\Omega$.

Assume that Ω is embedded in a cartesian domain $\tilde{\Omega}$, and f extended to $\tilde{\Omega}$ as a periodic function $\tilde{f}$. Let then $\tilde{u}$ solve the "periodic problem"

$$L\tilde{u} = \tilde{f} \qquad \text{in } \tilde{\Omega}$$

and u' the "homogeneous problem"

$$\begin{aligned} Lu' &= 0 \qquad \text{in } \Omega \\ \mathcal{B}(u') &= g - \mathcal{B}(\tilde{u}) \qquad \text{on } \Gamma. \end{aligned}$$

Then the solution u is given by

$$u = \tilde{u} + u'.$$

The main points associated with this algorithm are:

—The extension procedure ($f \longrightarrow \tilde{f}$), which should yield a very smooth extended function $\tilde{f}$. This point has been addressed in [8]. Assuming f sufficiently regular, it is based on an efficient solution of the constrained optimization problem,

$$\min |\Delta^p \tilde{f}\,|_{L^2_{per}(\tilde{\Omega})}, \qquad \tilde{f}|_{\Omega} = f,$$

where $L^2_{per}(\tilde{\Omega})$ is the space of the square integrable periodic functions in $\tilde{\Omega}$ and p a parameter characteristic of the extension procedure. For a better computational efficiency, an extension strip is generally used: f is only extended in a narrow strip around Ω, while the values of $\tilde{f}$ are set equal to zero outside Ω and the strip.

—The u' boundary value problem, which is solved with a boundary element method (BEM) requiring only the discretization of the boundary Γ, since the forcing term has been handled by the periodic problem.

First, in Section 2, we recall how the vorticity-stream function formulation of the incompressible Navier–Stokes equations can be handled using such an embedding approach. The crucial point of the calculation of the advection term, which must be accurately computed but also obtained in an efficient way, is revisited in Section 3, where a new algorithm is introduced. Furthermore, in the case of high values of the ratio Re/τ, Re being the Reynolds number and τ the time step, we propose in Section 4 an asymptotic version of the method, in which the BEM part of the algorithm is only applied to the Laplace equation; in that case all calculations of the BEM matrices entries may be analytic and a lot of simplifications and savings in time and memory storage are gained. Finally, to show the capabilities of the method in both its full and asymptotic versions, we consider in Section 5 the classical problem of the flow between two eccentric cylinders. The basic notions of potential theory required for a good understanding of the paper are given in Appendix.

2. ALGORITHM FOR THE ω-ψ FORMULATION OF THE NAVIER–STOKES EQUATION

In the the vorticity (ω)-stream function (ψ) formulation, the incompressible Navier–Stokes equations read

$$\begin{aligned} \frac{\partial \omega}{\partial t} + \vec{V} \cdot \nabla \omega &= \frac{1}{Re} \triangle \omega + F \\ \triangle \psi + \omega &= 0 \end{aligned} \tag{1}$$

with t for the time, $\vec{V} = (\frac{\partial \psi}{\partial y}, -\frac{\partial \psi}{\partial x})$ for the velocity vector, Re for the Reynolds number, and F for a given body force term.

The initial and boundary conditions must result from those imposed on the velocity. The initial vorticity is thus taken as the curl of the initial velocity, and Dirichlet boundary conditions on the velocity induce boundary conditions on the stream function and its normal outward derivative (ψ_Γ and $(\frac{\partial \psi}{\partial n})_\Gamma$), at least for a simply connected domain. The case of multi-connected domains is a little less straightforward, as discussed later in the text.

Using in time a finite difference scheme which takes into account explicitly the non-linear advection term and more or less implicitly the linear ones, at each time step we are led to solve the so-called generalized Stokes problem (GSP),

$$\begin{aligned} \triangle \omega - \sigma^2 \omega &= f \qquad \text{in } \Omega \\ \triangle \psi + \omega &= 0 \qquad \text{in } \Omega \\ \psi|_\Gamma &= \psi_\Gamma \\ \left.\frac{\partial \psi}{\partial n}\right|_\Gamma &= \left(\frac{\partial \psi}{\partial n}\right)_\Gamma, \end{aligned} \tag{2}$$

where σ and f depend on the considered scheme. For instance, for the AB/BE2 scheme (second order backward-Euler for the time derivative and linear Adams–Bashforth extrapolation for the advection term), at time index $n+1$,

$$\sigma^2 = \frac{3\,Re}{2\,\tau}$$

$$f = Re[(-4\omega^n + \omega^{n-1})/2\tau + 2(\vec{V} \cdot \nabla \omega)^n - (\vec{V} \cdot \nabla \omega)^{n-1} - F^{n+1}].$$

If the body-force term, the initial and boundary conditions are regular, and if the domain Ω is smooth (main restriction), the two-dimensional unsteady incompressible Navier–Stokes equations yield a regular solution (see, e.g., [12]). Then f is also regular and can be extended, as described in Section 1, in $\tilde{\Omega}$. But the straight application to the GSP of the embedding method described in the Introduction would require $\tilde{f}$ to have a zero mean value, which would add a constraint to the extension problem. To overcome this difficulty, the periodic problem is modified slightly as

$$\begin{aligned} \triangle \tilde{\omega} - \sigma^2 \tilde{\omega} &= \tilde{f} \qquad \text{in } \tilde{\Omega} \\ \triangle \tilde{\psi} + \tilde{\omega} &= \bar{\tilde{\omega}} \qquad \text{in } \tilde{\Omega}, \end{aligned} \tag{3}$$

where $\bar{\tilde{\omega}}$ stands for the mean value of periodic part of the vorticity. A $\delta\psi$ correction is then added to $\tilde{\psi}$, to take into account $\bar{\tilde{\omega}}$. It has to verify $\triangle \delta\psi = -\bar{\tilde{\omega}}$, e.g., $\delta\psi = -\frac{1}{2}\bar{\tilde{\omega}} x^2$.

The homogeneous problem then reads

$$\begin{aligned} \triangle\omega' - \sigma^2\,\omega' &= 0 \qquad \text{in } \Omega \\ \triangle\psi' + \omega' &= 0 \qquad \text{in } \Omega \\ \psi'|_\Gamma &= g_1 \\ \left.\frac{\partial\psi'}{\partial n}\right|_\Gamma &= g_2, \end{aligned} \tag{4}$$

where g_1 and g_2 are given by

$$\begin{aligned} g_1 &= \psi_\Gamma - (\tilde{\psi}|_\Gamma + \delta\psi|_\Gamma) \\ g_2 &= \left(\frac{\partial\psi}{\partial n}\right)_\Gamma - \left(\left.\frac{\partial\tilde{\psi}}{\partial n}\right|_\Gamma + \left.\frac{\partial\delta\psi}{\partial n}\right|_\Gamma\right). \end{aligned}$$

The solution of the GSP is obtained by superposition,

$$\begin{aligned} \psi &= \tilde{\psi} + \delta\psi + \psi' \\ \omega &= \tilde{\omega} + \omega'. \end{aligned}$$

The periodic problem is straightforward when it is solved in the Fourier spectral space, using a regular mesh for $\tilde{\Omega}$. In fact, $\tilde{\omega}$ and $\tilde{\psi}$ are evaluated from their modes which read, with obvious notations,

$$\begin{aligned} \hat{\tilde{\omega}}_k &= \frac{-\hat{\tilde{f}}_k}{|\vec{k}|^2 + \sigma^2} \\ \hat{\tilde{\psi}}_k &= \frac{\hat{\tilde{\omega}}_k}{|\vec{k}|^2}, \qquad |\vec{k}| \neq 0,\ \bar{\tilde{\psi}} = 0. \end{aligned} \tag{5}$$

For the homogeneous problem, to be solved, for the sake of efficiency, with only BEM solver of homogeneous scalar elliptic equations, the Poisson equation on ψ' must be transformed. This can be achieved by introducing the variable φ such as $\varphi = \sigma^2\psi' + \omega'$. Then, the homogeneous problem becomes

$$\begin{aligned} \triangle\omega' - \sigma^2\,\omega' &= 0 \qquad \text{in } \Omega \\ \triangle\varphi &= 0 \qquad \text{in } \Omega \\ \varphi|_\Gamma - \omega'|_\Gamma &= \sigma^2 g_1 \\ \left.\frac{\partial\varphi}{\partial n}\right|_\Gamma - \left.\frac{\partial\omega'}{\partial n}\right|_\Gamma &= \sigma^2 g_2. \end{aligned} \tag{6}$$

Now, one can use the fact that φ and ω' verify a Laplace and an homogeneous Helmholtz equation to solve the problem (6) without domain mesh. Many BEM algorithms are possible, but in any case, after discretization of the boundary Γ, one may write (see the Appendix)

$$\begin{aligned} \boldsymbol{\partial}_{\mathbf{n}}\boldsymbol{\omega}' &= A_h\boldsymbol{\omega}' \\ \boldsymbol{\partial}_{\mathbf{n}}\boldsymbol{\varphi} &= A_p\boldsymbol{\varphi}, \end{aligned} \tag{7}$$

where $\boldsymbol{\omega}'$, $\boldsymbol{\varphi}$, $\boldsymbol{\partial}_{\mathbf{n}}\boldsymbol{\omega}'$, and $\boldsymbol{\partial}_{\mathbf{n}}\boldsymbol{\varphi}$ are the vectors gathering the values of each variable and their normal derivatives at the boundary element nodes; A_h and A_p are the BEM boundary matrices for the Helmholtz and Laplace operators. In our numerical implementation, a collocation method is used with linear discontinuous elements so to enable jumps in the normal derivative (e.g., to support geometries having corners).

In discrete form, the boundary conditions provided by problem (6) become

$$\begin{aligned} \boldsymbol{\varphi} - \boldsymbol{\omega}' &= \sigma^2 \mathbf{g_1} \\ \boldsymbol{\partial}_{\mathbf{n}}\boldsymbol{\varphi} - \boldsymbol{\partial}_{\mathbf{n}}\boldsymbol{\omega}' &= \sigma^2 \mathbf{g_2}. \end{aligned} \tag{8}$$

Then using Eqs. (7), (8), and the definition of φ, the boundary vorticity is obtained as

$$\boldsymbol{\omega}' = \sigma^2 (A_h - A_p)^{-1} (A_p \mathbf{g_1} - \mathbf{g_2}). \tag{9}$$

Once $\boldsymbol{\varphi}$ and $\boldsymbol{\omega}'$ are known, one can evaluate ω', φ, and ψ' at the inner collocation points of Ω. This can be achieved using an indirect approach based on a single-layer potential formulation, as described in the Appendix. The adoption of this formulation is motivated by the fact that the integral kernel u_M^* is continuous when M passes through the boundary, so that near-wall evaluation of the solution is more accurate. Moreover, the numerical computation of the solution in the domain requires only one matrix of dimension $N_\Omega \times N$ (N, number of boundary collocation points; N_Ω, number of inner Fourier grid points) in contrast to the usual mixed integral formulation which requires two. However, the single-layer potential approach is to be used with care in the case of irregular geometries, because the resulting potential layer, μ, may be no longer regular.

3. COMPUTATION OF THE ADVECTION TERM

As it may be expected, the main difficulty of the present method lies in the determination of the non-linear term $(\vec{V} \cdot \nabla\omega)$ since it requires the evaluation of the solution derivatives, i.e., $\nabla\omega$ and $\vec{V} = (\frac{\partial\psi}{\partial y}, -\frac{\partial\psi}{\partial x})$. Indeed, as ω and ψ are given by superposition, their periodic and homogeneous parts should be differentiated independently. But as it is well known, calculations of derivatives by BEM are not straightforward [13].

Let us mention here that one can also evaluate the advection term without using the BEM. Indeed, once ω and ψ are obtained inside Ω, one can then find their extensions to $\tilde{\Omega}$: $\breve{\omega}$ and $\breve{\psi}$ such that $\breve{\omega}|_\Omega = \omega$ and $\breve{\psi}|_\Omega = \psi$. Then it's easy to differentiate in the Fourier space to obtain the advection term $(\vec{V} \cdot \nabla\omega)$. This approach was used in [9]. Nevertheless it suffers from a loss of regularity, especially near the boundary where the calculations of the derivatives are no longer accurate.

Thus a good accuracy is expected by differentiating independently the periodic and homogeneous parts of ω and ψ, but the difficulty comes from the differentiation, with respect to the space variables x_i, $i = 1, 2$, of ω' and φ which solve the homogeneous Helmholtz and Poisson problems.

One way would be to differentiate the basic BIE (boundary integral equation), but this yields hypersingular kernels which are difficult to handle numerically and requires considerable memory storage for the associated matrices. As it has been done for the solution, one

can also use the single-layer potential formulation to obtain, with the notations defined in Appendix,

$$(\nabla u)_M = (1 - c_M)\,\mu\vec{n} - \int_\Gamma \nabla u^*_M \mu\, ds. \tag{10}$$

Such an approach, which we used in [8], is to be preferred to the previous one, since ∇u^*_M does not yield hypersingular kernels. Nevertheless, the memory storage requirements are still important : one $N_\Omega \times N$ matrix for each $\frac{\partial u}{\partial x_i}$ derivative. Moreover, one serious difficulty arises from the discontinuous character of ∇u^*_M through the boundary, leading to the deterioration of the near-wall accuracy. In order to overcome these difficulties, sophisticated approaches, which basically rely on using a local Taylor approximation of the solution near the boundary, have been suggested, as in [14]. But although such methods have shown improvements in the overall accuracy, the obtained algorithms are usually highly complex, which in our case is not what we are looking for.

The approach proposed hereafter does not suffer from the mentioned drawbacks, i.e., accuracy near the boundary is obtained and high memory storage is not necessary. However, it requires more regularity on the computed solution. Coming back to the homogeneous Helmholtz equation, if the solution u is sufficiently regular then

$$\Delta u - \sigma^2 u = 0 \Longrightarrow \Delta\left(\frac{\partial u}{\partial x_i}\right) - \sigma^2\left(\frac{\partial u}{\partial x_i}\right) = 0.$$

One notices that once the trace of $(\frac{\partial u}{\partial x_i})$ is known, then $(\frac{\partial u}{\partial x_i})$ can be evaluated at the inner points of Ω in the same way as for the solution u. The improvement of the near-wall evaluation of the derivatives results, as for the solution, from the continuous character of the integral kernel u^*_M. Furthermore, no extra $N_\Omega \times N$ matrix is needed for inner point evaluation of the derivatives. The problem then resumes to find $(\frac{\partial u}{\partial x_i})_\Gamma$. This can be done once the normal and tangential derivatives of u on the boundary are known. The evaluation of the normal derivative of the solution is already dealt with as a result of the standard BEM and so what remains is to determine the tangential derivative. One obvious way to proceed is by finite differences, using in our implementation the fact that the solution u is assumed to be linear on each boundary element. But such a procedure shows a poor accuracy: the linear profiles assumed for u can only be justified as a mean to evaluate the integrals arising from the BEM.

Finally, the BEM algorithm that we suggest for computing the tangential derivative $(\frac{\partial u}{\partial s})_\Gamma$ is based on the following vectorial BIE, which results from a direct formulation and holds for both the Helmholtz or Laplace equation (with $\sigma = 0$),

$$c_M \nabla u_M = \int_\Gamma \left(\left(\sigma^2 u\, u^*_M + \nabla u \cdot \nabla u^*_M\right)\vec{n} - \frac{\partial u^*_M}{\partial n}\nabla u - \frac{\partial u}{\partial n}\nabla u^*_M \right) ds. \tag{11}$$

The proof is, e.g., given in [15]. In 2D context, it is then easy to obtain an integral equation for $\frac{\partial u}{\partial s}$. Indeed, the BIE (11) can be projected on the tangent to Γ at point M, to obtain

$$c_M \left(\frac{\partial u}{\partial s}\right)_M + \int_\Gamma \left(\vec{\tau}_M \cdot \left(\nabla u^*_M\right)^\perp\right)\frac{\partial u}{\partial s}\, ds = \int_\Gamma \sigma^2 (\vec{n} \cdot \vec{\tau}_M) u\, u^*_M\, ds - \int_\Gamma \left(\vec{\tau}_M \cdot \nabla u^*_M\right)\frac{\partial u}{\partial n}\, ds \tag{12}$$

with $(\nabla u_M^*)^\perp$ defined as the $\frac{\pi}{2}$ rotation of the vector ∇u_M^* and $\vec{\tau}_M$ as the unit vector tangent to Γ.

In the discrete frame work, such a BIE yields the matrix relation

$$H^s \boldsymbol{\partial}_\mathbf{s}\mathbf{u} = G^s \boldsymbol{\partial}_\mathbf{n}\mathbf{u} + \sigma^2 Q^s \mathbf{u}, \tag{13}$$

where the BEM integrals associated with the new obtained matrices H^s, G^s, and Q^s are related to the already evaluated integrals, so that no additional numerical quadrature is required [15].

By elimination of $\boldsymbol{\partial}_\mathbf{n}\mathbf{u}$, one can deduce $\boldsymbol{\partial}_\mathbf{s}\mathbf{u}$ from $\mathbf{u}$ as

$$\boldsymbol{\partial}_\mathbf{s}\mathbf{u} = Q\,\mathbf{u}, \tag{14}$$

where Q is defined as

$$Q = H^{s^{-1}}(G^s A + \sigma^2 Q^s).$$

To conclude this section, we test the accuracy of the proposed differentiation method by considering the following exact solution of the homogeneous Helmholtz equation,

$$u = \mathrm{I}_0\big(\sigma\sqrt{(\mathrm{x}-0.1)^2 + (\mathrm{y}-0.1)^2}\big),$$

where I_0 is the modified Bessel function of the first type and zero order. The domain Ω is chosen as the square $]-\frac{1}{2}, \frac{1}{2}[^2$ and $\sigma = 1$.

Figure 1a shows the variations of the tangential derivative computed by the proposed method and by finite differences. The corresponding errors are plotted in Fig. 1b. One notices how the jumps of $(\frac{\partial u}{\partial s})_\Gamma$ at the four corners of the domain are well described, and how the proposed method is very accurate in contrast to the finite difference approximation.

In Fig. 2, we check the derivative calculation inside the domain, by showing the errors on $(\frac{\partial u}{\partial x})$ along the diagonal $y = x$, $0 \le x \le \frac{1}{2}$. One notices that even in the vicinity of the corner, the calculation accuracy remains quite satisfactory. Such an accuracy is out of reach when using Eq. (10), which yields quite false results for x in the range [0.48, 0.5], as shown in [15].

The tests were made with 80 boundary elements of variable size ($N = 160$), by using, for each side of the square, a Chebyshev–Gauss–Lobatto distribution for the endpoints of the boundary elements.

4. ASYMPTOTIC VERSION OF THE EMBEDDING METHOD

Until now the value of the parameter σ^2 has been assumed arbitrary. However, in real practical simulations, this coefficient, $\sigma^2 \sim \frac{Re}{\tau}$, becomes generally high, typically $10^3 \le \sigma^2 \le 10^6$. With such a high value of σ, the fundamental solution of the Helmholtz equation has a very small support and thus gives rise, for the homogeneous Helmholtz equation, to solutions which are very confined at the boundary: the solution is almost negligible except in the vicinity of the boundary Γ where a layer occurs. As described now, one can take advantage of this to develop an asymptotic version of the method.

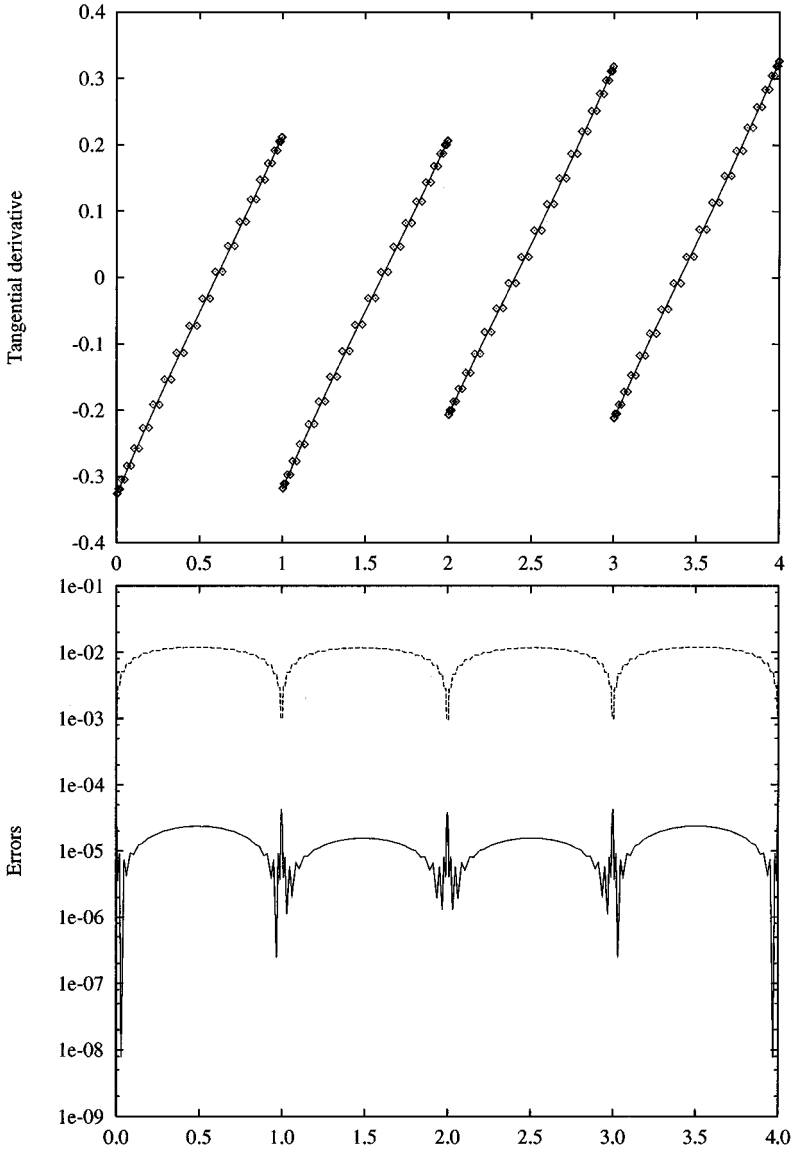

FIG. 1. (a) Tangential derivative computed with BEM and with finite differences (symbols) vs the curvilinear abscissa; (b) corresponding errors (BEM in full line and FD in dashed line).

Let us consider again the Dirichlet problem,

$$\begin{aligned} \Delta u - \sigma^2 u &= 0 \qquad \text{in } \Omega \\ u_{|\Gamma} &= u_\Gamma \end{aligned} \tag{15}$$

with $\sigma \gg 1$.

Suppose that Ω is such that the last equation develops boundary layers which do not interact (for instance, interaction may happen in the case of some non-simply connected

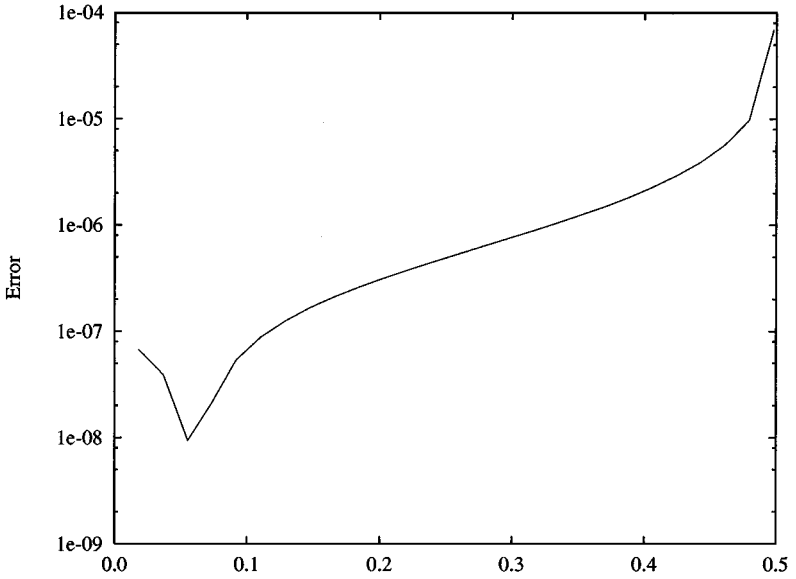

FIG. 2. Accuracy of $\frac{\partial u}{\partial x}$ along the diagonal of the square vs x.

domain). Once Eq. (15) is written in the Frénet local frame $(\vec{n}, \vec{\tau})$, it reads

$$\frac{\partial^2 u}{\partial n^2} + \kappa \frac{\partial u}{\partial n} + \frac{\partial^2 u}{\partial s^2} - \sigma^2 u = 0, \tag{16}$$

where κ stands for curvature.

Introduce the lengths δ_n and δ_τ which characterize the variations in the normal and tangent directions ($\delta_n \ll \delta_\tau$). Then with $\vec{n} = \delta_n \vec{n}'$ and $\vec{\tau} = \delta_\tau \vec{\tau}'$, Eq. (16) becomes

$$\frac{\partial^2 u}{\partial n'^2} + \delta_n \kappa \frac{\partial u}{\partial n'} + \left(\frac{\delta_n}{\delta_\tau}\right)^2 \frac{\partial^2 u}{\partial s'^2} - \delta_n^2 \sigma^2 u = 0. \tag{17}$$

This last equation shows that:

—The boundary layer thickness is $\mathcal{O}(\frac{1}{\sigma})$.

—The term $(\delta_n/\delta_\tau)^2(\partial^2 u/\partial s'^2)$ can be neglected.

—The term $\delta_n \kappa(\partial u/\partial n')$ can also be neglected if one supposes further that the curvature radius is sufficiently high.

With these approximations, the solution of (15) reads

$$u(d, s) = u_\Gamma(s) e^{-\sigma d}, \tag{18}$$

where d is the distance from the boundary. Thus the resulting boundary layer is of exponential type and one can deduce

$$\nabla u(d, s) \approx \sigma u_\Gamma(s) e^{-\sigma d} \vec{n}(s). \tag{19}$$

Especially, at the boundary,

$$\left.\frac{\partial u}{\partial n}\right|_\Gamma \approx \sigma u_\Gamma. \tag{20}$$

Such an equation shows that when the value of σ is high, the BEM operator A_h is approximately proportional to the $N \times N$ identity matrix: $A_h \approx \sigma \mathbf{1}_\Gamma$.

Coming back to the Navier–Stokes equation in the ω-ψ formulation, Eq. (9) can be drastically simplified by assuming

$$A_h - A_p \approx \sigma \mathbf{1}_\Gamma$$

which satisfies both the limiting case $\sigma = 0$ and $\sigma \gg 1$. In that case, Eq. (9) simplifies to

$$\boldsymbol{\omega}' = \sigma(A_p \mathbf{g_1} - \mathbf{g_2}). \tag{21}$$

In fact, when assuming $g_1 = 0$, so that $\omega = -\sigma g_2$, one recovers here the equation derived in [16] following another integral formulation.

Once $\boldsymbol{\omega}'$ is obtained, ω' and $\nabla\omega'$ are evaluated at the inner points of Ω using Eqs. (18) and (19). The rest of the algorithm is then applied unchanged. For instance, φ satisfies the Laplace Dirichlet problem,

$$\begin{aligned} \triangle\varphi &= 0 \qquad \text{in } \Omega \\ \varphi|_\Gamma - \omega'|_\Gamma &= \sigma^2 g_1 \end{aligned} \tag{22}$$

which is the only problem that has to be solved by the BEM.

The resulting advantages of the asymptotic version of the method are important:

—The preliminary calculations of the BEM matrix entries only relate to the Laplace equation. When using rectilinear boundary elements, all evaluations of integrals are then done analytically and so no numerical quadrature is needed.

—The preliminary calculations no longer depend on the coefficient σ, i.e., on the the Reynolds number and on the time step. Adaptability in the time step or variations in time of the Reynolds number then become possible.

5. FLUID FLOW BETWEEN TWO ECCENTRIC CYLINDERS

To validate the proposed algorithms we consider the problem of the flow between two eccentric cylinders of radius R_1 and R_2 ($R_1 < R_2$) and with eccentricity e defined as the distance between the two cylinders' centers. The case of the inner cylinder being rotating is considered. For this kind of flow, the clearance defined by $c = R_2 - R_1$ is chosen as the characteristic length.

For the sake of comparison, the geometry and flow parameters are identical to those given in [17]: $R_1 = 1$, $R_2 = 2$, $e = 0.5$, and $Re = 37.2$, the Reynolds number being based on the inner cylinder tangential velocity.

The main features of this flow are known to be controlled by the Taylor number defined as $Tn = Re\sqrt{c/R_1}$. When the inner cylinder is the one rotating, the flow remains two dimensional and laminar up to $Tn = 41.6$. Note that for the case considered $c = R_1$ and consequently $Tn = Re$.

As it is well known, the doubly connected feature of the geometry induces a difficulty when using the ω-ψ formulation: the value of the stream function can be taken to be arbitrary on one of the two cylinders, e.g., $\psi = 0$ on the fixed one, but the other value, then equal to the flowrate, has to be determined.

To overcome this difficulty, we proceed as in [17, 18]. The Navier–Stokes equations, written in the primitive variables and restricted at the boundary of the fixed cylinder ($\vec{V} = 0$), simplify to, with p for the pressure

$$Re\nabla p = \Delta\vec{V}. \tag{23}$$

For a divergence free field, $\Delta\vec{V} = -\nabla \times \nabla \times \vec{V}$, so that Eq. (23) becomes

$$Re\nabla p = \nabla\omega \times \vec{e}_z, \tag{24}$$

where $\vec{e}_z$ is the unit vector normal to the flow plane.

The projection of this equation on the tangential direction of the boundary Γ_2 of the outer cylinder yields

$$Re\frac{\partial p}{\partial s} = \frac{\partial \omega}{\partial n}. \tag{25}$$

Integrating this equation on Γ_2 gives

$$\int_{\Gamma_2} \frac{\partial \omega}{\partial n}\, ds = 0. \tag{26}$$

This equation is then used to determine the value $\alpha = \psi|_{\Gamma_1}$.

In the framework of the present embedding method, Eq. (26) becomes

$$\int_{\Gamma_2} \frac{\partial \omega'}{\partial n}\, ds = -\int_{\Gamma_2} \frac{\partial \tilde{\omega}}{\partial n} = \beta. \tag{27}$$

In order to calculate α, a function θ defined on Γ is introduced:

$$\theta(M) = \begin{cases} 1 & \text{if } M \text{ on } \Gamma_1 \\ 0 & \text{otherwise.} \end{cases}$$

Then the basic equation for $\boldsymbol{\omega}'$ reads

$$\boldsymbol{\omega}' = S(A_p(\mathbf{g}_1' + \alpha\boldsymbol{\theta}) - \mathbf{g}_2), \tag{28}$$

where $\mathbf{g}_1'$ is evaluated assuming $\psi|_\Gamma = 0$ and where $S = \sigma^2(A_h - A_p)^{-1}$ or $S = \sigma\mathbf{1}_\Gamma$, for the full and asymptotic versions of the method, respectively.

When put in discrete form, Eq. (27) is used to obtain α,

$$\alpha = \frac{\beta - \mathcal{R}A_h S(A_p\mathbf{g}_1' - \mathbf{g}_2)}{\mathcal{R}A_h S A_p\boldsymbol{\theta}}, \tag{29}$$

where $\mathcal{R}$ is the discrete integration operator on Γ_2.

For the asymptotic version, this equation simplifies to

$$\alpha = \frac{\beta - \mathcal{R}\sigma^2(A_p\mathbf{g}_1' - \mathbf{g}_2)}{\mathcal{R}\sigma^2 A_p\boldsymbol{\theta}} \tag{30}$$

since $S \approx A_h \approx \sigma\mathbf{1}_\Gamma$.

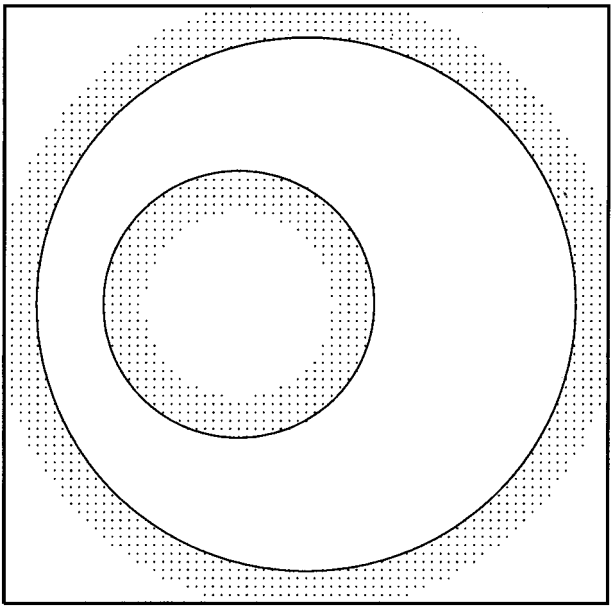

FIG. 3. Schematic of the geometry and visualisation of the grid-points of the extension band.

Using the AB/BE2 scheme mentioned in Section 2, simulations have been conducted for both the full and asymptotic versions of the method.

Figure 3 shows a schematic of the geometry, embedded in the square $]-2.24, 2.24[^2$, with the distribution of the grid-points inside the extension strip. From our experience of the method, the thickness of the extension strip must be at least 5 Fourier grid-points and the embedding domain $\tilde{\Omega}$ may fit the union of Ω and this strip. The extension parameter was taken equal to $p = 3$. Higher values are to be avoided, because independently of the

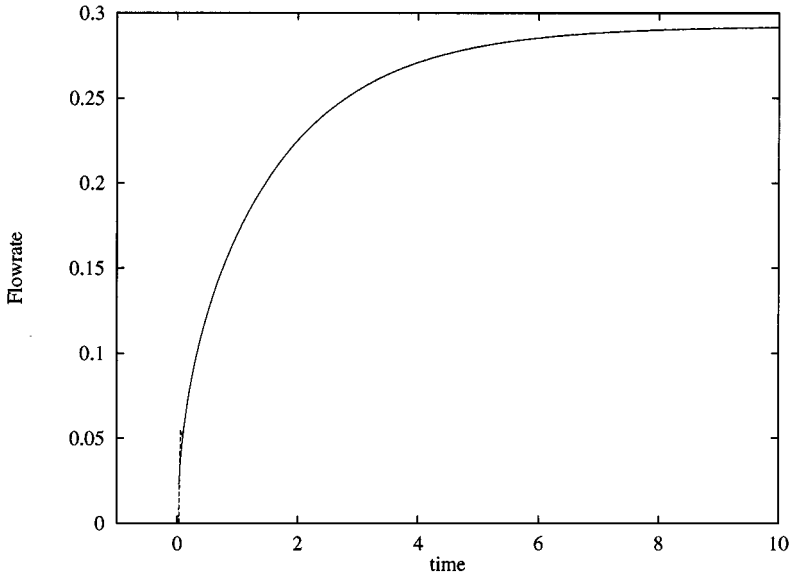

FIG. 4. Flowrate vs time, computed with the full and asymptotic (dashed line) versions of the method.

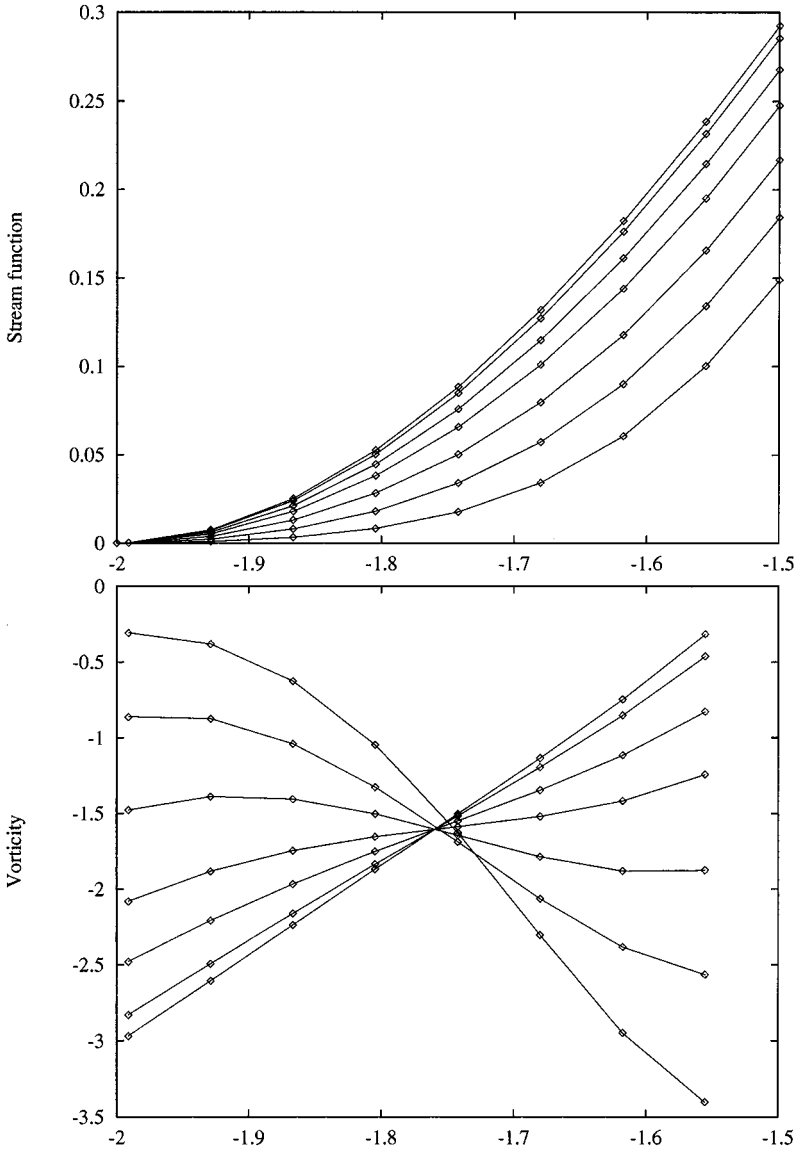

FIG. 5. Stream function and vorticity in the narrow gap, as computed at different times with the full and asymptotic (symbols) versions of the method.

GSP source term f, numerical difficulties may arise with the extension procedure, which involve terms like $|\vec{k}|^{2p}$ [8]. In any case one has to check that the periodic variable Fourier spectra show satisfactory decays. For the Fourier grid we used $N_F = 72$ Fourier points in each direction. Then one gets $N_\Omega = 2406$ inner grid-points. For the boundary element mesh we used 300 elements, i.e., $N = 600$ boundary collocation points (400 on the big cylinder and 200 on the small one), in such a way that the boundary element size approximately equaled the Fourier mesh step. The calculations were done with the time-step $\tau = 3.10^{-2}$, i.e., $\tau \approx 0.5\tau_{CFL}$ (τ_{CFL}, the Courant–Friedrichs–Lewy critical time-step). For this value of τ, with $Re = 37.2$, one gets $\sigma \approx 43.1$.

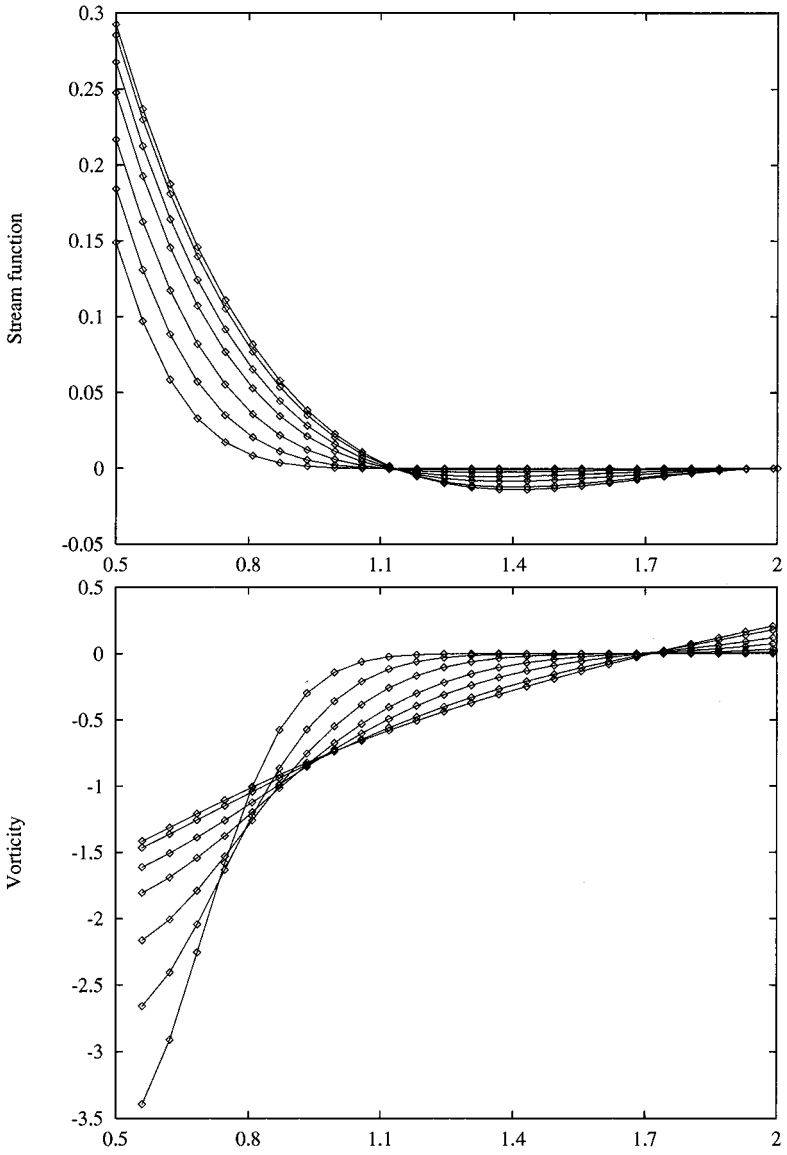

FIG. 6. Stream function and vorticity in the wide gap, as computed at different times with the full and asymptotic (symbols) versions of the method.

Figure 4 shows the flowrate, as computed with both the expressions 29 and 30. On such a graphic it is not possible to discern the two corresponding curves, except for $t \approx 0$, essentially because at the first time-step the approximate formula yields an erroneous (but well understood) result: $\alpha = 0$.

In order to compare the full and asymptotic approaches, the profiles of the vorticity and of the stream function, in the narrow and wide gap between the two cylinders, are shown in the Figs. 5 and 6. These profiles are given at the different times, $t = \{0.75, 1.2, 1.8, 2.7, 3.75, 6., 25.\}$. At the wall of the inner cylinder ($x = -1.5$ and $x = 0.5$), both the vorticity and the stream function are increasing with time. Notice that the vorticity values are only given where ω has been computed, i.e., at the grid-points of the Fourier mesh, whereas

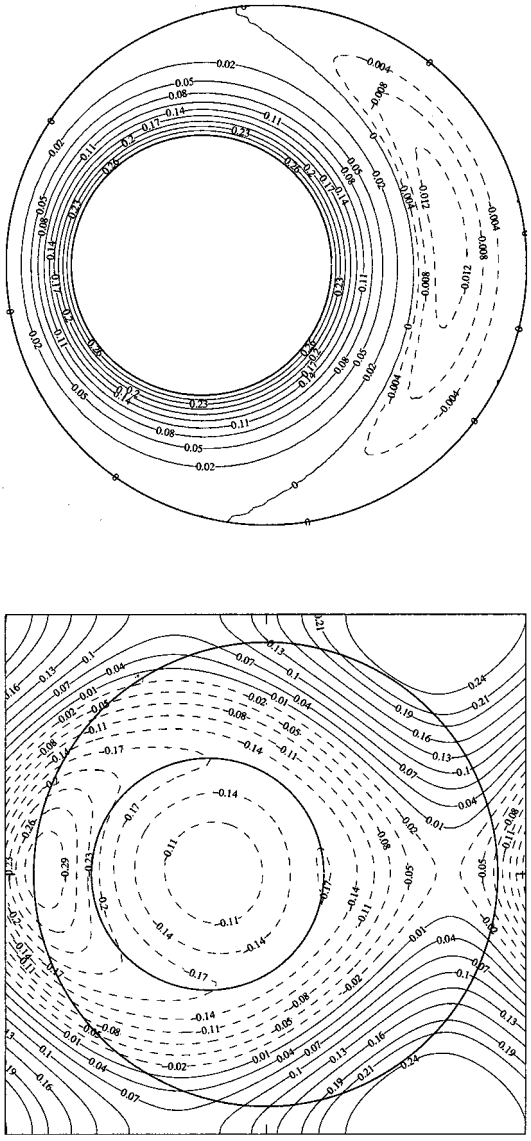

FIG. 7. Stream function and its periodic part.

the boundary values of the stream function are well known: $\psi = \alpha$ and $\psi = 0$, along the inner and outer cylinder, respectively. Once again, the agreement appears to be very good, since the differences, which are less than 10^{-3} in relative values, cannot be discerned on the figures.

To get insight into the method, the final time solution of ψ and ω is shown in Figs. 7 and 8 along with their periodic parts $\tilde{\psi}$ and $\tilde{\omega}$. These results have been obtained with the asymptotic version of the method, but as shown in Fig. 9 the results are quite similar with the full one. As expected, ω and $\tilde{\omega}$ are nearly the same, except close to the boundary where the homogeneous part of the vorticity ω' is no longer negligible. This behavior is not followed by the stream function and its periodic part.

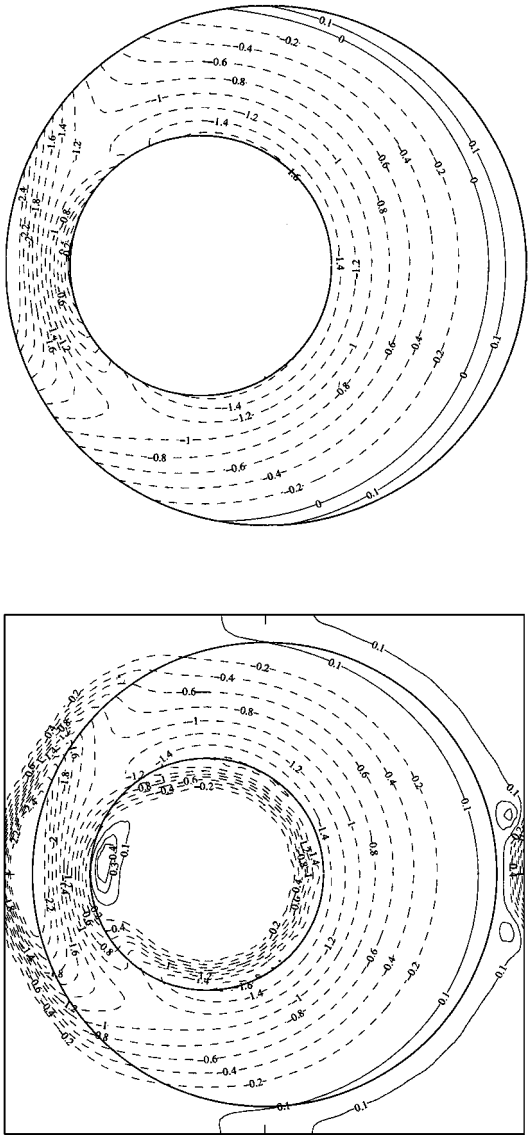

FIG. 8. Vorticity and its periodic part.

Finally, let us mention that our results agree well with those presented in [17]. Especially the two stagnation points on the outer cylinder are located at about ± 98.6 degree and the separation stream line intersects the horizontal axis at about $x \approx 1.16$.

6. CONCLUSION

The embedding method proposed in [8, 9] has been applied to the incompressible Navier–Stokes equations in the $\omega - \psi$ formulation. Especially we have focused on the computation of the advection term, by using here an approach showing some major advantages: near-wall accuracy calculations and low memory storage requirements. Moreover, an asymptotic version of the method has been proposed, in such a way that the BEM is only used for

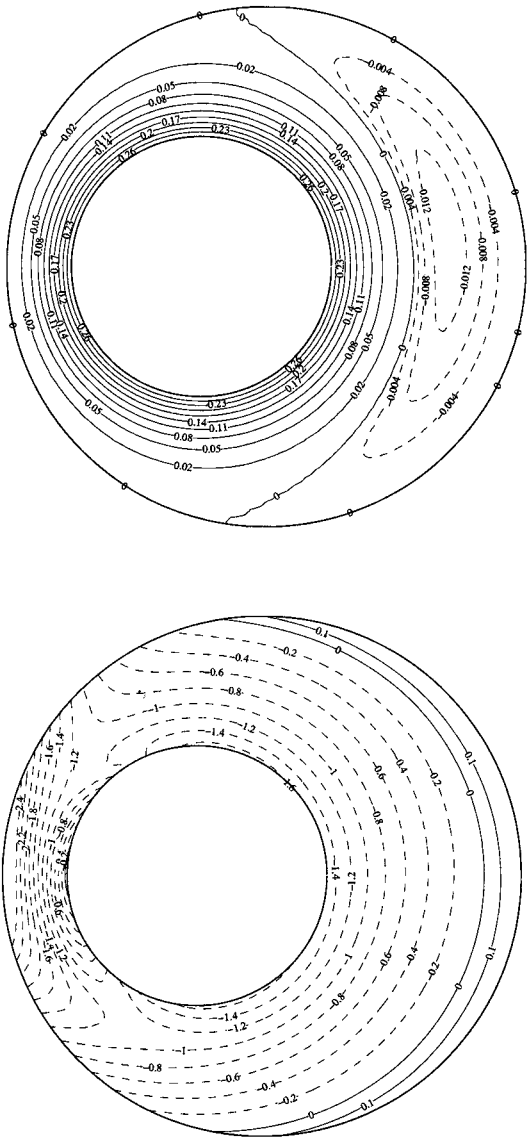

FIG. 9. Stream function and vorticity, computed with the full version of the method.

solving the Laplace equation. By considering the classical problem of the flow between two eccentric cylinders, we have pointed out that the proposed embedding method can produce satisfactory results and constitutes, especially in its asymptotic version, an efficient way to solve the Navier–Stokes equations in complex geometries, at least at moderate Reynolds numbers.

APPENDIX

The homogeneous Poisson and Helmholtz equations, say $L(u) = 0$, with L for the Laplacian or for the elliptic Helmholtz operator $(\Delta - \sigma^2)$, can be recast into a boundary

integral equation (BIE) involving no domain integrals,

$$c_M u_M + \int_\Gamma u \frac{\partial u^*_M}{\partial n}\, ds = \int_\Gamma u^*_M \frac{\partial u}{\partial n}\, ds,$$

where M is a point in $\bar{\Omega}$, u_M the value of u at point M, c_M a coefficient equal to 1 if M is in Ω, and such as $0 < c_M < 1$ if M is on Γ ($c_M = 0.5$, if Γ is smooth at M). The so-called fundamental solution u^*_M is the Green function such as in an unbounded domain,

$$L(u^*_M) + \delta_M = 0,$$

where δ_M is the Dirac distribution at point M:

—for the 2D Poisson equation, $u^*_M = \frac{-1}{2\pi} \ln(\rho)$
—for the 2D elliptic Helmholtz equation, $u^*_M = \frac{1}{2\pi} K_0(\sqrt{\sigma}\rho)$

with ρ being the distance to point M and where K_0 is the modified Bessel function of the second kind and zero order, which presents, for $\rho = 0$, a logarithmic singularity and which exponentially vanishes at infinity.

The discrete equations are obtained by discretizing the boundary into boundary elements and by expressing the BIE at their boundary nodes. This can be done in several ways, but in any case, with $\mathbf{u}$ and $\boldsymbol{\partial}_\mathbf{n}\mathbf{u}$ for the vectors of the boundary node values of the numerical approximations of u and $\frac{\partial u}{\partial n}$, one gets a matricial relation of the form (see, e.g., [19]),

$$H\mathbf{u} = G\boldsymbol{\partial}_\mathbf{n}\mathbf{u}$$

or, with $A = G^{-1}H$, $\boldsymbol{\partial}_\mathbf{n}\mathbf{u} = A\mathbf{u}$.

In the framework of an "indirect approach," one has also the single-layer potential formulation, which states that there exists μ such that, up to a constant in case of the Laplacian operator,

$$u_M = \int_\Gamma u^*_M \mu\, ds.$$

In discrete form, this equation yields for the boundary node values

$$\mathbf{u} = G\boldsymbol{\mu}.$$

Similarly, for the internal points,

$$\mathbf{u}_\Omega = G_\Omega \boldsymbol{\mu} = G_\Omega G^{-1}\mathbf{u},$$

where $\mathbf{u}_\Omega$ stands for the values of u at the collocation points inside Ω and where G_Ω is a matrix which only depends on the geometry. In case of the Laplace equation the additive constant is calculated from the Gauss condition,

$$\int_\Gamma \mu\, ds = 0.$$

ACKNOWLEDGMENT

We are very grateful to J. M. Lacroix for his helpful and quite necessary technical support.

REFERENCES

1. B. L. Buzbee, F. W. Dorr, J. George and G. H. Golub, The direct solution of the discrete Poisson equation on irregular regions, *SIAM J. Numer. Anal.* **8**, 722 (1971).
2. G. P. Astrakmantsev, Methods of fictitious domains for a second order elliptic equation with natural boundary conditions, *U.S.S.R. Comput. Math. Math. Phys.* **18**, 114 (1978).
3. M. Briscolini and P. Santangelo, Development of the mask method for incompressible unsteady flows, *J. Comput. Phys.* **84**, 57 (1989).
4. P. N. Vabishchevitch, *The Method of Fictitious Domains in Problems of Mathematical Physics*, Izdatel'stvo Moskovskogo Univ., Moscow, 1991.
5. C. Atamian, G. V. Dinh, R. Glowinski, Jiwen He, and J. Periaux, On some embedding methods applied to fluid dynamics and electro-magnetics, *Comput. Methods Appl. Mech. Eng.* **91**, 1271 (1991).
6. R. Glowinski, T. W. Pan, and J. Periaux, A fictitious domain method for external incompressible viscous flow modeled by Navier–Stokes equations, *Comput. Methods Appl. Mech. Eng.* **112**, 133 (1994).
7. R. Glowinski, T. W. Pan, and J. Periaux, A Lagrange multiplier fictitious domain method for the Dirichlet problem: Generalization to some flow problems, *J. Industr. Appl. Math.* **12**, 87 (1995).
8. M. Elghaoui and R. Pasquetti, A spectral embedding method applied to the advection-diffusion equation, *J. Comput. Phys.* **125**, 464 (1996).
9. M. Elghaoui and R. Pasquetti, A spectral embedding method for the incompressible Navier–Stokes equations, in *Congrès ECCOMAS '96* (Wiley, New York, 1996), p. 124.
10. W. Borchers, F. K. Hebeker, and R. Rautmann, A boundary element spectral method for nonstationary viscous flows in 3 dimensions, in *Finite Approximations in Fluid Mechanics*, Notes of Numer. Fluid. Mech. (Hirschel, Vieweg & Son, Germany, 1986), p. 14.
11. H. Gründemann, A general procedure transferring domain integrals onto boundary integrals in BEM, *Eng. Anal. Boundary Elements* **6**, 214 (1989).
12. R. Temam, *Navier–Stokes Equations* (North-Holland, Amsterdam/New York/Oxford, 1977).
13. Hajime Igarashi and Toshhisa Honma, Strategies for the accurate computation of potential derivatives in boundary elements method: Application to two-dimensional problems, *J. Comput. Phys.* **119**, 244 (1995).
14. V. Sladek and J. Sladek, Non-singular boundary integral representation of potential field gradients, *Int. J. Numer. Methods Eng.* **33**, 1181 (1992).
15. M. Elghaoui, Thesis, University of Nice-Sophia Antipolis, France, 1998.
16. Y. Achdou and O. Pironneau, A fast solver for Navier–Stokes equations in the laminar regime using mortar finite element and boundary element methods, *SIAM J. Numer. Anal.* **32**(4), 985 (1995).
17. D. R. Sood and H. G. Elrod Jr., Numerical solution of the incompressible Navier–Stokes equations in doubly-connected regions, *AIAA J.* **12**(5), 636 (1974).
18. P. M. Gresho, Some current CFD issues relevant to the incompressible Navier–Stokes equations, *Comput. Methods Appl. Mech. Eng.* **87**, 201 (1991).
19. C. A. Brebbia, J. C. F. Telles, and L. C. Wrobel, *Boundary Element Techniques, Theory and Applications in Engineering* (Springer-Verlag, Berlin, 1984).